Compact rubidium-stabilized multi-frequency reference source in the 1.55-µm region

Renaud Matthey,* Florian Gruet, Stéphane Schilt, and Gaetano Mileti

Laboratoire Temps-Fréquence, Institut de Physique, Université de Neuchâtel, Bellevaux 51, 2000 Neuchâtel, Switzerland
*Corresponding author: renaud.matthey-de-lendroit@unine.ch

Combining light modulation and frequency conversion techniques, a compact and simple frequency-stabilized optical frequency comb spanning over 45 nm in the 1.56-µm wavelength region is demonstrated. It benefits from the high-frequency stability achievable from rubidium atomic transitions at 780 nm probed in a saturation absorption scheme, which is transferred to the 1.56-µm spectral region via a second-harmonic generation process. The optical frequency comb is generated by an electro-optic modulator enclosed in a Fabry–Perot cavity that is injected by the fundamental frequency stabilized laser. Frequency stability better than 2 kHz has been demonstrated on time scales between 1000 s and 2 days both at 1560 nm, twice the rubidium wavelength, and for a comb line at 1557 nm.

OCIS codes: (120.4800) Optical standards and testing; (120.3930) Metrological instrumentation; (140.3425) Laser stabilization; (300.6460) Spectroscopy, saturation.

To predict future climate evolutions, the knowledge of carbon dioxide (CO_2) exchanges between the atmosphere and the Earth's lands and oceans must be improved, especially by better identifying CO_2 sinks and sources [1]. In this context, a satellite-borne CO_2 integrated-path differential-absorption lidar (IPDA) system [2] is being considered by space agencies [3]. To achieve the scientific goals of such a mission, feasibility studies [1,4] defined relatively stringent requirements on the lidar instrument and, in particular, on the frequency stability of the laser transmitter. A wavelength of 1572 nm is envisaged for a satellite mission and is already used to detect CO_2 with ground-based and airborne lidar instruments [5]. At this wavelength, a target frequency stability—in terms of Allan deviation—has been determined as better than 200 kHz at 7 s and below 20 kHz ($<10^{-10}$ fractional stability) for integration times ranging from 700 s up to the envisaged 3-year operational lifetime of the mission [6]. While the requirement on the short-term stability has already been fulfilled, the long-term value reveals challenging.

At low pressure and room temperature, the Doppler-broadened linewidth of CO_2 transitions at 1.57 µm is ~350 MHz (FWHM). This value is more than four orders of magnitude larger than the targeted frequency stability. Furthermore, the line strength of the CO_2 transitions is as low as $1.8 \cdot 10^{-23}$ cm^{-1}/(molecule $\cdot$ cm^{-2}) at 1572 nm, requiring an optical pathlength of several meters at least to reach a sufficient absorption signal for laser frequency locking with the necessary stability. In this way, fractional frequency stability of about $3 \cdot 10^{-11}$ was obtained at the center of a CO_2 absorption line at 1572 nm for integration time up to 1000 s [7]; a 17-m pathlength multipass cell combined with a frequency modulation technique was used. If the laser shall be operated at a detuned frequency from the absorption line center (typically up to 3 GHz), an electro-optical modulator (EOM) generating side-bands can be implemented.

Saturated absorption spectroscopy enables circumventing Doppler broadening and reaching much narrower linewidth of a molecular or atomic transition. Acetylene (C_2H_2) transitions are commonly used in the optical range of 1.51–1.54 µm for laser stabilization and as wavelength references. Sub-MHz linewidth was reached for saturated C_2H_2 transitions, but it generally requires placing the gas sample in a Fabry–Perot (FP) cavity to enhance the optical power and increase the absorption pathlength at the same time. Rubidium (Rb) shows two to three orders of magnitude lower saturation intensity than C_2H_2. Doppler-free linewidth of 20 MHz or less can be observed at 780 nm and 795 nm for optical powers as low as 200 µW with an optical pathlength of a couple of centimeters. These easily achievable sub-Doppler lines make the Rb D2 transition at 780 nm particularly favorable as a frequency reference in the 1.56-µm optical telecommunication region through second-harmonic generation (SHG) [8,9], and for lasers probing CO_2 lines at 1.57 µm. Rb-based frequency-stabilized laser heads were developed, demonstrating fractional frequency stability better than $1 \cdot 10^{-11}$ and $2 \cdot 10^{-12}$ at all timescales between 1 s and 1 day for a distributed feedback (DFB) laser [10] and an extended-cavity diode laser [11], respectively. Two-photon transition of rubidium atoms is also used for frequency standards at 1556 nm, demonstrating high stability at the level of 10^{-13} or better between 10 and 1000 s [12], however in a less simple and compact setup.

An optical frequency comb (OFC) with frequency-controlled lines allows bridging the gap between two spectral regions and avoiding locking a laser to a weak absorption line. A laser can then be locked to any frequency between two OFC lines with an offset-locking technique [13]. Self-referenced OFCs from mode-locked lasers provide a coherent link between the microwave and optical domains. Such combs are entirely controlled by only two radio frequencies (RF), the pulse repetition rate and the carrier-envelope offset frequency, which can both be stabilized to external microwave references [14]. However, this type of OFC system is still complex and generally requires table-top instrumentation, although large efforts are realized toward robustness and simplicity of use. OFCs can also be produced from a high-quality factor micro-resonator pumped by a continuous-wave

(cw) laser via nonlinear optical parametric frequency conversion [15]. While such approach is promising, especially in terms of comb spanning spectrum (hundreds of nm) and compactness, stability at the 20-kHz level over days has not been reported yet to the best of our knowledge. An OFC can further be generated by placing an EOM inside a FP optical cavity for resonant modulation enhancement of a cw laser field leading to the generation of a multitude of high-order sidebands [16]. The line spacing of this so-called FP-EOM corresponds to the EOM modulation frequency, typically in the GHz regime. Based on this principle, an optical frequency comb generator (OFCG) was demonstrated in the 1.5-µm region with a broad comb spectrum spanning over 4 THz (32 nm) [17]; a waveguide-type OFCG was developed with the advantages of compactness and high modulation index [18].

In this Letter, we demonstrate an OFC acting as a stable optical frequency reference in the 1.54–1.58-µm range, in particular around 1572 nm, a wavelength adequate to monitor CO_2 atmospheric concentration. An Rb transition is used as absolute frequency reference. The system fulfils the targeted performances requirements on time scales up to weeks for CO_2 monitoring instrumentation, with promises over longer time scale. Additionally, it offers a high potential for coherent detection in optical fiber telecommunication systems or gas-sensing and high-resolution spectroscopic measurements. System compactness and simplicity were retained as key specifications in view of future field and aircraft deployment, and possible evolution toward space instrumentation.

The realized system is sketched in Fig. 1. A DFB laser emitting at 1560 nm is frequency-stabilized to an Rb saturated absorption transition at 780 nm through second-harmonic generation. Part of the fundamental frequency laser beam feeds an OFCG to produce a stable frequency comb. The complete setup relies on polarization-maintaining (PM) fibers, as the OFCG and SHG devices are pigtailed and polarization-sensitive, as well as heterodyne beat-note detection units. The all-fiber connectorized configuration provides flexibility in the experimental set-up but may induce spurious etalon fringes effects.
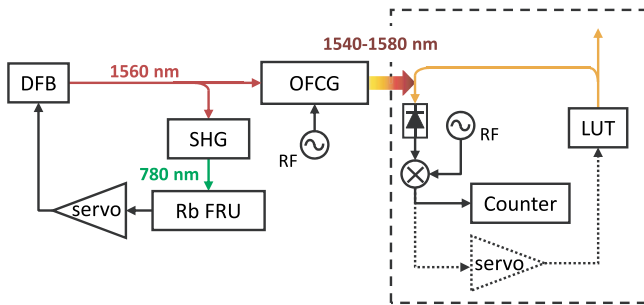

Fig. 1. Schematics of the instrumental setup. DFB, distributed feedback laser; SHG, second-harmonic generator; Rb FRU, rubidium frequency reference unit; OFCG, optical frequency comb generator; RF, radio-frequency oscillator. LUT, laser under test. The part enclosed in the dashed box shows how the laser system can be used either to measure the frequency stability of a LUT, or to offset-lock it to a line of the generated optical frequency comb (dotted line chain).

A telecom-grade fiber-coupled DFB laser (Emcore) emitting at 1560.5 nm is used as a laser source. It can deliver up to 80 mW of optical power. A linewidth of 1.0 MHz was retrieved from measurement of the fre-quency noise spectrum based on the concept of the β—separation line [19]. An external fiber optical isolator immediately follows the laser output. Part of the laser power is launched into an SHG module (NTT) that generates radiation at 780 nm for frequency locking. The module is composed of a fiber-coupled 5-cm-long periodically poled lithium niobate (PPLN) waveguide. A maximum conversion efficiency of $\backsim$300 %/W for the complete module, including the fiber insertion losses, was measured, so that 670 µW of optical power at 780 nm are generated from 15 mW of 1.56-µm light. As the band-width of the SHG module (98 GHz FWHM) largely exceeds the laser modulation amplitude used for frequency stabi-lization (typically 1–2 MHz), related output power varia-tions are negligible (0.03% at maximum).

The 780-nm light is directed into an in-house frequency reference unit (FRU) with extremely similar features as previously reported [10]. The laser light probes Rb atoms in a sub-Doppler saturated absorption scheme at 780 nm (D2 line) with a single retroreflected beam. Narrow Doppler-free resonances (direct transitions and crossovers) of 15 MHz (FWHM) are obtained in a small home-built evacuated cylindrical cell (10-mm diameter by 19-mm length) filled with a vapor of enriched [87]Rb isotope. The technology of such glass-blown Rb vapor cell is established from Rb atomic clocks for ground and space-borne applications such as global navigation satellite systems (GNSS). Owing to its small dimensions, it hardly causes optical interference fringes, or the corresponding free spectral range (FSR) is much larger than the line-width of the resonance used for laser locking purpose, in contrast to the situation encountered with multipass cells. In addition, it does not exhibit detrimental Fresnel reflections or surface modes unlike hollow-core fiber gas cells, which constitute other factors degrading the frequency stability of a locked laser. The FRU sensitivity to the parameters most affecting the frequency stability [11] is minimized; the optical components are mounted on a thermally stabilized baseplate to prevent dealignment; the Rb cell is also independently thermally stabilized at 40°C, and it is mounted in a magnetically-shielded package. Laser frequency-locking to an Rb transition is achieved by dithering the laser frequency at 50 kHz through direct injection current modulation combined with a phase-sensitive detection to generate the error signal. The applied 1.6-MHz modulation amplitude (corresponding to a normalized modulation index of ~0.2) suits the linewidth of a lidar transmitter laser (typ. $\geq$ 10 MHz) for CO_2 spectroscopy.

The OFCG used in our setup (OptoComb) consists of a polarization-sensitive waveguide FP phase-EOM with fiber-coupled input and output ports. The optical cavity takes place between two mirrors coated on the wave-guide facets. The cavity has an FSR of 2.5 GHz and a finesse of 60. It is temperature-stabilized to ensure proper long-term operation. The EOM is modulated at the 4th harmonic of the FP cavity FSR (10 GHz) to produce a comb spectrum with the widest span. A frequency synthesizer phase-locked to a hydrogen maser (replaceable

by a GPS-referenced Rb atomic clock for compactness and mobility purposes) is used as an RF modulation source and ensures a highly stable frequency interval between the comb lines. The frequency ν_n of the nth optical comb line (n being a positive or negative integer) is given by $\nu_n = \nu_{cw} + n \cdot f_m$, ν_{cw} and f_m being the frequency of the cw DFB laser and the RF modulation, respectively. The frequency stability of the comb lines is thus mainly governed by the cw laser. As shown in Fig. 2, the generated optical comb spans over 45 nm, encompassing CO_2 absorption lines at 1.57 μm. As the laser frequency is modulated for its stabilization to the Rb transition, the frequency of each comb line is similarly modulated. This situation offers the advantage that a slave laser can be simply and easily offset-locked to a comb mode using the method described in Ref. [13] without requiring any further frequency modulation, as the beat note between the slave laser and the selected comb line is indeed modulated by the comb line dithering.

The frequency stability of the laser system was measured at different wavelengths by heterodyne detection with various external optical frequency references. The beat-note frequencies were measured using frequency counters referenced to a hydrogen maser whose frequency is tracked and compared to a high-performance GNSS receiver. The stability of the frequency-doubled master laser was first evaluated at 780 nm by picking up a portion of the optical power at the output of the SHG module and heterodyning it with an Rb-stabilized reference laser that demonstrates relative frequency stability better than $1 \cdot 10^{-11}$ at all timescales from 1 s up to 1 day [10]. The impact of the laser stabilization is clearly seen in Fig. 3 in comparison with the free-running regime. The fractional frequency stability of the locked laser always remains below $4 \cdot 10^{-11}$ (corresponding to 8-kHz absolute stability at 1560 nm). Influence of the laboratory air conditioning cycle is discernible at 700 s, while the instability at around 20–30 s originates from etalon-induced interferences involving a fiber splice at the output of the SHG module. The achieved frequency stability depends on the particular transition used to lock the laser. It slightly degrades at short term (up to 100 s) when the laser is locked to the direct $F = 2 \rightarrow 3$ transition instead of the cross-over CO21-23, as a result of its lower signal-to-noise ratio. The signal of the direct transition is weaker and slightly broader, which makes the impact of interferometric fringes stronger. However, the direct
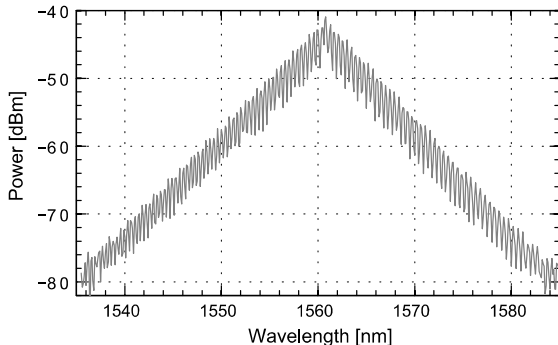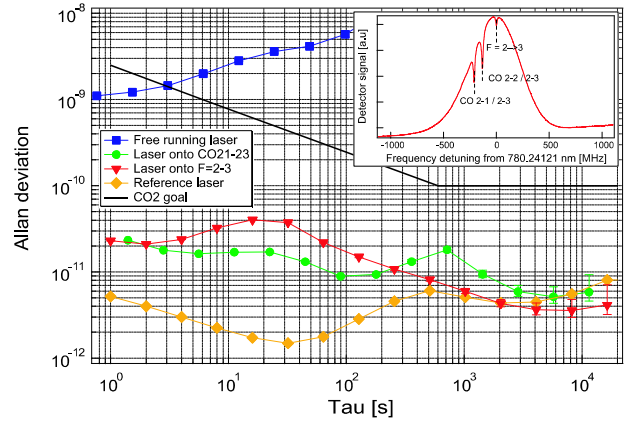

Fig. 3. Fractional frequency stability of the beat note between the frequency-doubled DFB laser and a 780-nm reference laser. Blue ■: free-running laser; green •: laser locked to Rb D2 cross-over CO21-23; red ▼: laser locked to $F = 2 \rightarrow 3$ transition; yellow ◆: beat note between two identical reference lasers. Inset: Rb D2 absorption lines at 780 nm ($F = 2$ hyperfine ground state) recorded with the cell assembly. Direct transition and cross-overs (CO) are indicated.

transition is less sensitive to changes of the underlying Doppler-broadened spectrum that result from temperature variations of the Rb vapor as it lies at the center of the Doppler profile, whereas the cross-overs stand on the side. Therefore, the medium- and long-term stabilities (above 100 s) are improved for the direct transition, which was then used in the subsequent measurements.

The frequency stability was also assessed at 1560 nm by beating a fraction of the DFB laser output power against a commercial Er-fiber frequency comb (MenloSystems). This reference comb provides a grid of absolute and stable optical frequencies resulting from its full stabilization (i.e., both repetition rate and carrier envelope offset frequencies) onto the aforementioned hydrogen maser. The high-fractional-frequency stability of the H-maser ($<4 \cdot 10^{-14}$ for integration times longer than 10 s) makes negligible the contribution of the reference comb to the instabilities of the beat-note frequencies. Simultaneously to 1560 nm, the stability of the frequency-doubled master laser was measured at 780 nm against the reference Rb-stabilized laser head. Finally, in a distinct set of measurements, the frequency stability of one line of the OFCG was assessed by heterodyning with an auxiliary narrow-linewidth (<100 kHz) semiconductor laser operating at 1557.36 nm, i.e., 3.12 nm apart from the OFCG seeding laser wavelength. The auxiliary laser was phase-locked to the reference Er-fiber comb to ensure its long-term stability. Even if the OFCG FP cavity was not locked to the frequency of the seeding 1560-nm laser [20], it remained sufficiently stable to generate a comb spectral width larger than 45 nm during the almost 7-day duration of the measurement performed at 1557 nm.

An excellent agreement is obtained between the fractional frequency stabilities measured at all wavelengths (780, 1560, 1557 nm) as shown in Fig. 4. The comb stability at 1557 nm faithfully reproduces the result of the 1560-nm laser, demonstrating no deterioration in the comb generation, at least within 3 nm from the 1560-nm master laser. A maximal fractional Allan deviation of

Fig. 2. Measured spectrum of the optical comb obtained when modulating the OFCG at 10 GHz with 26 dBm of RF power.
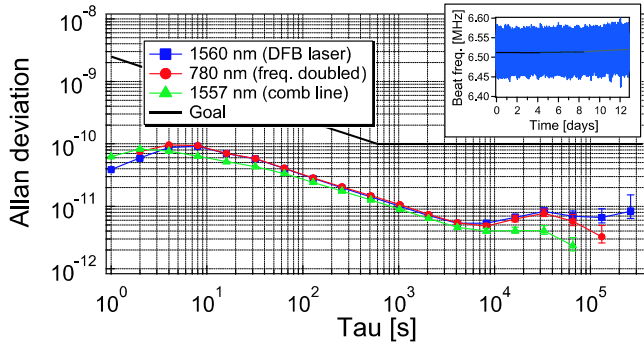
Fig. 4. Fractional frequency stabilities of the beat-note signals between various components of the laser system and different optical references. Blue ■: DFB laser at 1560 nm versus Er-fiber reference comb; red •: frequency-doubled DFB laser versus 780-nm laser head; green ▲: OFCG comb versus 1557-nm reference laser. Black solid line: aimed stability for CO_2 detection. Inset: time series of the beat-note frequency at 1560 nm with drifts over 4-day periods (black, grey, and light grey lines).

$1 \cdot 10^{-10}$ (corresponding to 20-kHz absolute frequency stability at 1572 nm) is achieved between 1- and 10-second integration time, improving down to below $1 \cdot 10^{-11}$ (2 kHz) between 1,000 and 200,000 s, about ten times better than the targeted value for CO_2 monitoring. During the 12 days of the full measurement performed at 1560 nm, the frequency excursion remained within a range of 150 kHz (see inset in Fig. 4). The drift over suc-cessive periods of 4 days varies as –90 Hz/day, 60 Hz/ day, and 1300 Hz/day (±36 Hz/day), not indicating any constant drift over weeks. The observed long-term frequency variations are linked to the slowly fluctuating laboratory background temperature. Some margins for amelioration still exist in the achieved frequency stabil-ities. For instance, the frequency stability at 1 s of the locked 1560-nm laser might be improved by a factor of four based on the short-term signal-to-noise ratio limit calculated from the detection noise power spectral den-sity and the discriminator slope of the error signal [21]. The main reason arises from the presence of multiple fibers and fiber-couplers/splitters in the stabilization and beat-note measurement setups. This effect is evidenced by the slight degradation of the short-term stability at 780 nm and 1560 nm displayed in Fig. 4 in comparison to the 780-nm stability reported in Fig. 3. By means of the reference comb, we measured the frequency of the 1560-nm laser four times in three months, unlocking the laser several times while still operating the system in nominally identical conditions. The frequency stayed within 25 kHz around 192 114 057.628 MHz, 27 kHz above half the value reported by Ye *et al.* [22] for the corre-sponding Rb D2 direct $F = 2 \rightarrow 3$ transition used to lock the laser. The locking point reproducibility, in particular when switching the system on and off, was however not systematically evaluated.

In conclusion, we have demonstrated that the frequency stability obtained from an Rb-stabilized laser source at 780 nm based on a saturation absorption scheme can be transferred with high fidelity to an optical frequency comb operating in the 1.56-µm region and spreading over 45 nm. Developed around waveguide-based optical devices, a centimeter-scale Rb cell and a DFB laser, the fiber-coupled system is kept compact and simple. The frequency stability of the comb was measured to be below 20 kHz up to 10 s integration time and below 2 kHz between 1,000 and 200,000 s. The developed system may serve as a long-term stable optical frequency reference for spectroscopy applications, in particular for CO_2 sensing, or in modern optical telecommunication applications involving coherent detection.

References

1. F.-M. Bréon and P. Ciais, Comput. Geosci. **342**, 412 (2009).
2. G. Ehret, C. Kiemle, M. Wirth, A. Amediek, A. Fix, and S. Houweling, Appl. Phys. B **90**, 593 (2008).
3. ESA, Report for Assessment, SP-1313/1 (2008).
4. J. Caron, Y. Durand, J.-L. Bezy, and R. Meynart, in *Proceedings of Lidar Technologies, Techniques and Measurements for Atmospheric Remote Sensing* **V** (SPIE, 2009), paper 74790E.
5. J. Abshire, H. Riris, C. Weaver, J. Mao, G. Allan, W. Hasselbrack, and E. Browell, Appl. Opt. **52**, 4446 (2013).
6. A. Fix, R. Matthey, A. Amediek, G. Ehret, F. Gruet, C. Kiemle, V. Klein, G. Mileti, J. Pereira do Carmo, and M. Quatrevalet, "Investigations on frequency and energy refer-ences for a space-borne integrated path differential absorp-tion lidar," in *Proceedings of the International Conference on Space Optics*, Tenerife, Spain (2014).
7. K. Numata, J. Chen, S. Wu, J. Abshire, and M. Krainak, Appl. Opt. **50**, 1047 (2011).
8. A. Bruner, V. Mahal, I. Kiryuschev, A. Arie, M. Arbore, and M. Fejer, Appl. Opt. **37**, 6410 (1998).
9. S. Masuda, A. Seki, and S. Niki, Appl. Opt. **46**, 4780 (2007).
10. F. Gruet, M. Pellaton, C. Affolderbach, T. Bandi, R. Matthey, and G. Mileti, "Compact and frequency stabilized laser heads for rubidium atomic clocks," in *Proceedings of the International Conference on Space Optics*, Ajaccio, Corsica (2012), paper 0048.
11. C. Affolderbach and G. Mileti, Rev. Sci. Instr. **76**, 073108 (2005).
12. M. Poulin, C. Latrasse, D. Touahri, and M. Têtu, Opt. Commun. **207**, 233 (2002).
13. S. Schilt, R. Matthey, D. Kauffmann, C. Affolderbach, G. Mileti, and L. Thévenaz, Appl. Opt. **47**, 4336 (2008).
14. R. Holzwarth, T. Udem, T. Hänsch, J. Knight, W. Wadsworth, and P. Russell, Phys. Rev. Lett. **85**, 2264 (2000).
15. P. Del'Haye, A. Schliesser, O. Arcizet, T. Wilken, R. Holzwarth, and T. Kippenberg, Nature **450**, 1214 (2007).
16. T. Kobayashi, T. Sueta, Y. Cho, and Y. Matsuo, Appl. Phys. Lett. **21**, 341 (1972).
17. M. Kourogi, K. Nakagawa, and M. Ohtsu, IEEE J. Quantum Electron. **29**, 2693 (1993).
18. T. Saitoh, M. Kourogi, and M. Ohtsu, IEEE Photon. Technol. Lett. **7**, 197 (1995).
19. G. Di Domenico, S. Schilt, and P. Thomann, Appl. Opt. **49**, 4801 (2010).
20. S. Xiao, L. Hollberg, and S. Diddams, Opt. Lett. **34**, 85 (2009).
21. T. Bandi, C. Affolderbach, C. E. Calosso, and G. Mileti, Electron. Lett. **47**, 698 (2011).
22. J. Ye, S. Swartz, P. Jungner, and J. Hall, Opt. Lett. **21**, 1280 (1996).